

Changes in North Sea storm surge conditions for four transient future climate realizations

Lidia Gaslikova · Iris Grabemann · Nikolaus Groll

Received: 20 October 2011 / Accepted: 3 July 2012 / Published online: 1 August 2012
© Springer Science+Business Media B.V. 2012

Abstract Storm surges in the North Sea are one of the threats for coastal infrastructure and human safety. Under an anthropogenic climate change, the threat of extreme storm surges may be enlarged due to changes in the wind climate. Possible future storm surge climates based on transient simulations (1961–2100) are investigated with a hydrodynamical model for the North Sea. The climate change scenarios are based on regionalized meteorological conditions with the regional climate model CCLM which is forced by AR4 climate simulations with the general circulation model ECHAM5/MPIOM under two IPCC emission scenarios (SRES A1B and B1) and two initial conditions. Possible sea level rise in the North Sea is not taken into account. The analysis of future wind-induced changes of the water levels is focused on extreme values. Special emphasis is given to the southeastern North Sea (German Bight). Comparing the 30-year averages of the annual 99 percentiles of the wind-induced water levels between the four climate realizations and the respective control climates, a small tendency toward an increase is inferred for all climate change realizations toward the end of the twenty-first century. Concerning the German Bight, the climate change signals are higher for the North Frisian coastal areas than for the East Frisian ones. This is consistent with an increase in frequency of strong westerly winds. Considering the whole time series (1961–2100) for selected areas, this tendency is superimposed with strong decadal fluctuations. It is found that uncertainties are related not only to the used models and emission scenarios but also to the initial conditions pointing to the internal natural variability.

Keywords Climate change · Storm surge heights · Extreme events · North Sea

L. Gaslikova · I. Grabemann · N. Groll (✉)
Institute of Coastal Research, Helmholtz-Zentrum Geesthacht, Centre for Materials and Coastal Research, Max-Planck-Str. 1, 21502 Geesthacht, Germany
e-mail: nikolaus.groll@hzg.de

L. Gaslikova
e-mail: lidia.gaslikova@hzg.de

1 Introduction

Anthropogenic climate change, as described in the Intergovernmental Panel on Climate Change (IPCC) Fourth Assessment Report (AR4), may cause long-term changes in the atmospheric pattern and, thus, in the wind, wave and storm surge conditions of the world ocean that could have significant impacts on the coasts and human activities. Parts of the densely populated and highly industrialized coasts of the North Sea, which is the principal area of interest in the present study, are below or slightly above today's mean sea level and are protected by various coastal defenses. These defenses as well as offshore activities and busy shipping routes in the North Sea itself are highly vulnerable to storms with their high water levels and associated waves, which are a major threat. Thus, the investigation of potential changes (trends) in storm surge climate is important to allow precautionary planning.

Based on scenario experiments of different lengths, climate change impact studies on future storm surge conditions were performed for chosen parts of the ocean such as the North Atlantic (e.g. Debernard and Røed 2008) and smaller areas like, e.g., the Adriatic Sea (e.g. Lionello et al. 2003), the Irish Sea (e.g. Brown et al. 2010), or the North Sea (e.g. Lowe and Gregory 2005; Woth et al. 2006).

Storm surge climate depends strongly on the meteorological conditions and those differ significantly when various future development scenarios are considered. Additionally, the same scenario simulated with different global/regional circulation models can lead to considerable differences in the atmospheric and consequently storm surge climate (e.g. Beniston et al. 2007). Moreover, the same scenario and circulation model can provide quite a variety of future atmospheric conditions due to internal natural system variability (e.g. Sterl et al. 2009). These uncertainties were partly addressed in the studies of the past decade. These studies comprise different analysis time horizons and a wide spectrum of models and scenarios. Such, Debernard et al. (2002) used 20-year time slices based on one circulation model and scenario (+1 % CO₂ per year, IPCC IS92a) and concluded that high percentiles of storm surge will not change significantly. Later, Debernard and Røed (2008) considered additional scenarios (Special Report on Emission Scenarios (SRES) A1B, A2 and B2) and circulation models and found an increase of about 6–10 % for the high storm surge percentiles for the south-eastern part of the North Sea. Lowe and Gregory (2005) used the same scenarios and 30-year time slices but applied different methodology and analyzed 50-year return periods instead of high percentiles. They came to the conclusion that according to the considered scenarios, the return values will increase at the end of the twenty-first century by 0.6–0.7 m in the German Bight.

The studies from Woth (2005) and Woth et al. (2006) were based on 30-year time-slice simulations with various combinations of 2 global and 4 regional circulation models, and two scenarios (SRES A2, B2). Despite the scenario-induced and model-related uncertainties, there was agreement among the different realizations that the high percentiles of storm surge heights increase in the German Bight toward the end of the twenty-first century. With the increasing computer power and computational resources in the recent years, the studies turned their attention to the transient runs (2001–2100) and greater amount of realizations with the aim to investigate rather the system internal natural variability than the uncertainties due to different scenarios and models. The studies from Sterl et al. (2009) and Howard et al. (2010) focused on the southwestern North Sea and storm surge return value as a prognostic variable, according to the coastal protection requirements. Based on 17-member ensembles for A1B SRES scenario and different circulation models in the two studies, they found no changes in the storm surge return values

beyond natural variability for the southern North Sea for the second half of the twenty-first century. Brown et al. (2011) investigate the monthly and seasonal skew surge heights in transient simulations based on A1B scenarios for the Liverpool Bay and found only few significant changes.

For the water level simulations, described in this study, a set of four transient global climate scenarios over 140 years (1961–2100) within the AR4 simulated with the general circulation model ECHAM5-MPIOM1 (European Centre Hamburg Version5/ Max Planck Institute-Ocean Model Version1 (Röckner et al. 2003; Marsland et al. 2003)) and down-scaled for the European continent and the NorthEast Atlantic with the regional climate model COSMO-CLM (COntortium for Small-scale MOdeling model—in CLimate Mode (Rockel et al. 2008; Hollweg et al. 2008)) was used for the atmospheric boundary conditions. This set comprises varying assumptions of future atmospheric composition (concentration of greenhouse gases, aerosols, etc. due to different future emissions) as well as the effects of unforced internal natural variability. To show a range of possible changes due to different emissions, the two scenarios A1B and B1 (AR4) (Houghton et al. 2001; Nakicenovic and Swart 2000) were taken into account for the twenty-first century. While the scenario A1B focuses on rapid global economic growth with well-balanced energy sources, the scenario B1 orients toward global environmental sustainability. The reference climate using observed emissions (1961–2000) for comparison was generated for two different initial conditions to incorporate the internal natural system variability.

In the present study, this set of four transient climate realizations was applied to dynamically simulate and analyze potential future changes in the storm surge conditions together with their temporal development from 2001 to 2100 in the North Sea for the first time. Special emphasis is given to the southeastern part of the North Sea, in particular the German Bight. The climate change signals derived from these climate realizations enlarge the ensemble for the North Sea storm surge scenarios, and thus further describe the range of scenario-induced uncertainties toward the end of the twenty-first century. Moreover, it provides an additional insight into the natural internal variability.

A rise in mean water level as well as future changes in today's topography were not taken into account in the simulations. The spatial resolution of the hydrodynamic model (12.8 km) is relative coarse for mapping the topographical highly variable near-shore and Wadden areas of the North Sea, and the simulations are most reliable for the deeper parts of the North Sea with water depths greater than 10 m. In the deeper parts, an expected sea level rise can be linearly superimposed on the wind-induced water levels (e.g. Lowe and Gregory 2005; Sterl et al. 2009; Howard et al. 2010).

2 Methodology

2.1 Models and simulations

To simulate water level and current fields, the hydrodynamical model TRIM-NP (Nested and Parallelized (Kapitza 2008; Kapitza and Eppel 2000) version of the three-dimensional finite difference Tidal Residual Intertidal Mudflat (TRIM) model (developed by Casulli and Cattani 1994)) was used in a 2D mode. The model solves the Reynolds-averaged Navier-Stokes equations on a regular Arakawa-C grid. For the simulations presented here, Cartesian coordinates with a spatial resolution of 12.8 km were used without nesting in this case. Flooding and drying of near-shore points were enabled. The model domain covers the North Sea and the adjacent parts of the northeastern North Atlantic to the north and west of

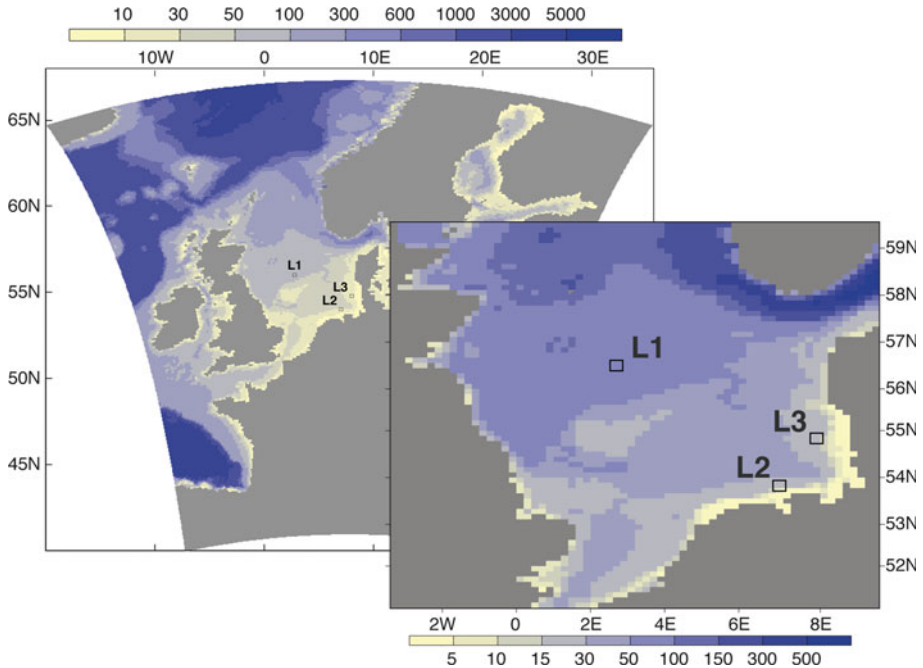


Fig. 1 Model domain of the hydrodynamic model TRIM-NP with the topography (water depth in m) together with the investigated area of the North Sea. The locations of three selected areas are marked by rectangles

Great Britain (Fig. 1). On the lateral boundaries, astronomical tides are considered as the only water-level variations. The boundaries are located sufficiently far away from the area of interest (southeastern North Sea) to allow the generation of realistic wind-induced surges and the consideration of the tide–surge interaction in the interior. The tidal signal was obtained from the fine element solutions (FES) tidal atlases (Lyard et al. 2006).

As atmospheric forcing, the hydrodynamic model requires 10 m height wind and mean sea level pressure (SLP) fields. For that, the hourly wind and 3-hourly SLP fields from the COSMO-CLM regionalizations (18 km \times 18 km resolution) of the global ECHAM5-MPIOM simulations (1.8° \times 1.8° horizontal resolution) for the two control climates C20_1 and C20_2 (1961–2000) and for the four future climate scenarios A1B_1, A1B_2, B1_1 and B1_2 (2001–2100) were used. The underscores 1 and 2 are related to the different initial conditions for the global simulations.

The hydrodynamic simulations were initialized at January 1, 1960, with the water level from the FES dataset. This initial state is sufficiently far in the past to be forgotten by the model in the time period of interest. Today’s or reference conditions are represented by “control simulations” (1961–2000). Possible future conditions in case of global warming are represented by “climate realizations” (2001–2100). In the following, the different water level simulations with the hydrodynamical model and their results will be referred to as indicated in Fig. 2. For each of the six simulations, hourly values for the water level were stored at every grid point. The results were used to calculate extreme storm surge statistics.

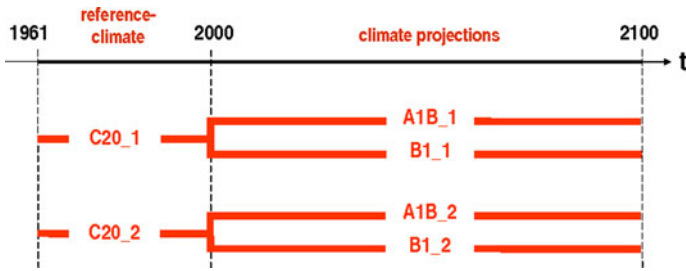


Fig. 2 Layout and timeline of the forcing: combinations of control (C20) and emission scenarios (A1B and B1) and initial conditions 1 and 2 used as driving data for the hydrodynamic model. The six output data sets of the TRIM-NP simulations are named with respect to the six driving data sets

To extract the storm surge component of the water level, an additional “tide-only” 140-year simulation (1961–2100) was performed using only the tidal signal at the open model boundaries as a driving force. The storm surge heights were subsequently derived by subtracting the “tide-only” simulation water levels from the “complete” control and scenario simulation water levels.

2.2 Statistical analysis

In the following, the discussion is concentrated on storm surge height and number and intensity of extreme events. Wind speed and direction representing the primary variables that determine storm surge behavior are included in the analysis. Future changes in storm surge conditions are analyzed spatially for time slices. The temporal variability is investigated for chosen areas, two of them located in the German Bight (Fig. 1). Since severe surge conditions have the largest implications for many sectors, such as coastal protection, offshore constructions or shipping, the analysis is limited to extreme conditions.

Annual upper percentiles P_{si}^{xn} of wind speed and storm surge height were calculated for every grid point x in the data set and for each year n from 1961 to 2100. $i = 1,2$ denotes the two different initial conditions and $s = A, B, C$ gives the different scenarios (A,B: emission scenarios A1B and B1, C: control “scenario” C20). Changes in the upper percentiles are considered to be a relatively robust measure for changes in the statistics of extreme events. These percentiles were averaged over 30-year time slices for e.g. 1961–1990 and 2071–2100: P_{si}^x .

The climate change signal Δ_{si}^x is defined as the difference between the value P_{si}^x in the climate change simulation ($s = A, B$) and the value from the corresponding control simulation P_{Ci}^x :

$$\Delta_{si}^x = P_{si}^x - P_{Ci}^x \tag{1}$$

The 30-year reference period P_{Ci}^x is given as average of the annual percentiles P_{Ci}^{xn} over the years 1961 to 1990, if not stated otherwise.

For a further, more detailed analysis of the climate signals in wind and storm surge conditions, 140-year long area-averaged time series were extracted for selected areas (Fig. 1). The results for these chosen areas with an extent of approximately 650 km² (4 grid cells) each will be presented.

For the area-averaged time series of storm surge height and wind speed, annual upper percentiles P_{si}^{an} for each of the simulations have been calculated. The 30-year averages over

1961–1990 of the two control simulations (P_{Ci}^a , $a = \text{area } 1, 2 \text{ or } 3$ and $i = 1, 2$) were used as thresholds for exceedance frequencies. The frequency, N_{si}^{an} , of extreme surges represents the number of exceedances over the threshold values P_{Ci}^a in hours per year n .

Each realization of the climate change signals remains equally likely. To get possibly more reliable results for the changes in wind speed and storm surge height, also the mean of the four climate projections has been calculated, mentioned as *ensemble mean* in the following.

Linear trends from 1961 to 2100 for annual 99 percentile and maximum surges for the areas L2 and L3 have been investigated for the four realisations and the ensemble mean. Additionally, 50-year return values of the annual maximum water levels and surge heights have been calculated for the two reference simulations (1961–2000) and for the four projections (2001–2100) as well as for the mean of the reference simulations and the mean of the projections for the same areas. For this, generalized extreme value (GEV) distributions have been fitted to the time series.

In addition, changes in the wind directions have been analyzed for strong winds (wind speed ≥ 17.2 m/s (8 beaufort)). The wind directions were divided into 30° segments from $15^\circ\text{--}45^\circ$ to $345^\circ\text{--}15^\circ$ (where $0^\circ/360^\circ$ corresponds to the north) and the frequency with which storms were coming from a particular sector has been counted. Changes in the frequency distributions between reference and scenario simulations display whether and how the dominant event wind directions could change in a specific area. Such changes could have different impact on the different coastal regions of the North Sea.

All shown changes and confidence intervals are tested for a statistical significance level of 95 % with either the Student's t test or with a bootstrapping method. Note that the Student's t test is appropriate for normal distributed variables; percentiles as mainly discussed here are generally not normally distributed. However, the Student's t test is a commonly used method and is used for comparability to other studies, and after the central limit theorem, the mean of several non-normal distributed variables converts to a normal distribution. Hence, a Student's t test is also used for testing the significance of the difference between two 30-year means of the annual 99 percentiles. Beside using the Student's t test, a bootstrapping approach was used to derive the confidence interval as this technique is independent from the parameter distribution.

3 Results

In this section, common features and differences in the climate change signals from the aforementioned simulations will be discussed. The presentation of the climate change signals will be limited to the area of interest, the North Sea. Changes in the parts of the North Atlantic which were included in the simulations to incorporate external surges during storms will not be discussed. First, results for 30-year long time slices (2071–2100) will be presented, and then, those for 140-year long time series at chosen locations will be described. The focus is on extreme conditions given by high percentiles (99 and above) and the 50-year return value.

3.1 Control versus historical climate

As long-term water-level observations from the tide gauges are only available for locations very near to the North Sea coasts, a hindcast simulation with high spatial resolution (Weisse and Pluess 2006) was used to test how close the water-level statistics from the

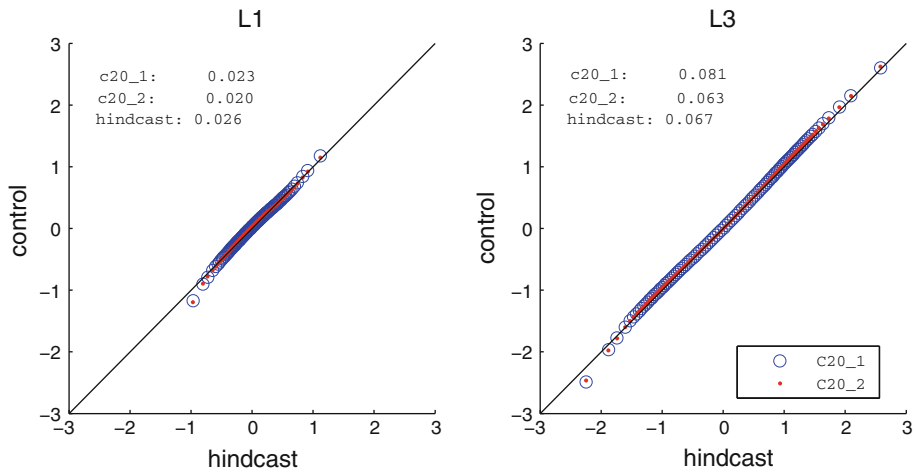


Fig. 3 Mean annual percentiles of water levels in meters at L1 (left) and L3 (right) over 1961–2000 from the hindcast and 2 control simulations (C20). Additionally, the numbers show the variance in meters over 40 years of the 99.9 percentile for each of the three simulations

control simulations are to real present-day climate. Figure 3 shows the comparison of the mean annual percentiles (1961–2000) obtained from the hindcast and the two control simulations for two locations in the German Bight (L3) and far off-shore in the North Sea (L1). These locations represent quite good the situation in the larger areas around. It can be seen that the percentiles from both control simulations are very close to each other when the entire period is considered, although they differ on the interannual scale, as it will be discussed later (Sect. 3.3). It also can be inferred that the control simulation statistics are generally in good agreement with the hindcast for both locations. There is a tendency of a slight underestimation of low water and overestimation of high water extremes by the control simulations. But, as has been mentioned by Weisse and Pluess (2006), the hindcast itself overestimates the low water extremes when compared to measurements, so the control simulations do not go farther from the real climate statistics than the hindcast. Also, the interannual variability of water-level percentiles is close for the three presented datasets. For example, the variance of the annual mean 99.9 percentiles for both control simulations lies within 0.5 cm around the hindcast variance for the area with low tidal range and within 1.5 cm for the high tidal range regions (Fig. 3). This analysis demonstrates that the two control climates used as references for future climate change impacts is in agreement with the results from the hindcast simulation and thus has a resemblance with the real climate.

3.2 Spatial distributions of the climate change signals

3.2.1 Wind speed and direction

As the surface wind is the main forcing factor for storm surges in the North Sea and changes in extreme wind conditions can help to explain changes in the extreme storm surge level, the 99 percentile of the annual 10 m height wind speed was analyzed. The 99 percentile is a good measure of storminess, because this percentile reaches about 18 m/s

near the North Sea coasts. This is just above eight beaufort (17.2 m/s) which is a storm benchmark.

Figure 4 shows the differences between the four climate projections for the 30-year time slice 2071–2100 and the corresponding control climate for 1961–1990 for the mean annual 99 percentile. A1B_1 (upper left panel) shows higher wind speed over the whole North Sea. Statistically significant (95 % level) changes ranging up to +0.7 m/s in the southern North Sea. Differences in the northern North Sea are smaller (+0.2 m/s), statistically not significant and vanish toward the north. Similar changes are found for B1_1 (upper right panel) with statistically significant values up to +0.4 m/s in the southern parts of the North Sea and the German Bight. A decrease in future wind speed (−0.2 m/s) is found for small areas along the British coast and toward the north.

For the realizations with initial condition 2, changes for the end of the century are generally smaller and less statistically significant compared to those based on initial condition 1. In A1B_2 (lower left panel), maximum statistically significant changes in wind speed (+0.4 m/s) occur in southern parts of the North Sea and are only up to +0.2 m/s in the German Bight. Compared to A1B_1, larger areas in the northern North Sea show negative deviations with −0.5 m/s near the Norwegian coast in A1B_2. B1_2 shows similar, but almost no statistically significant changes in the north (−0.6 m/s) and the

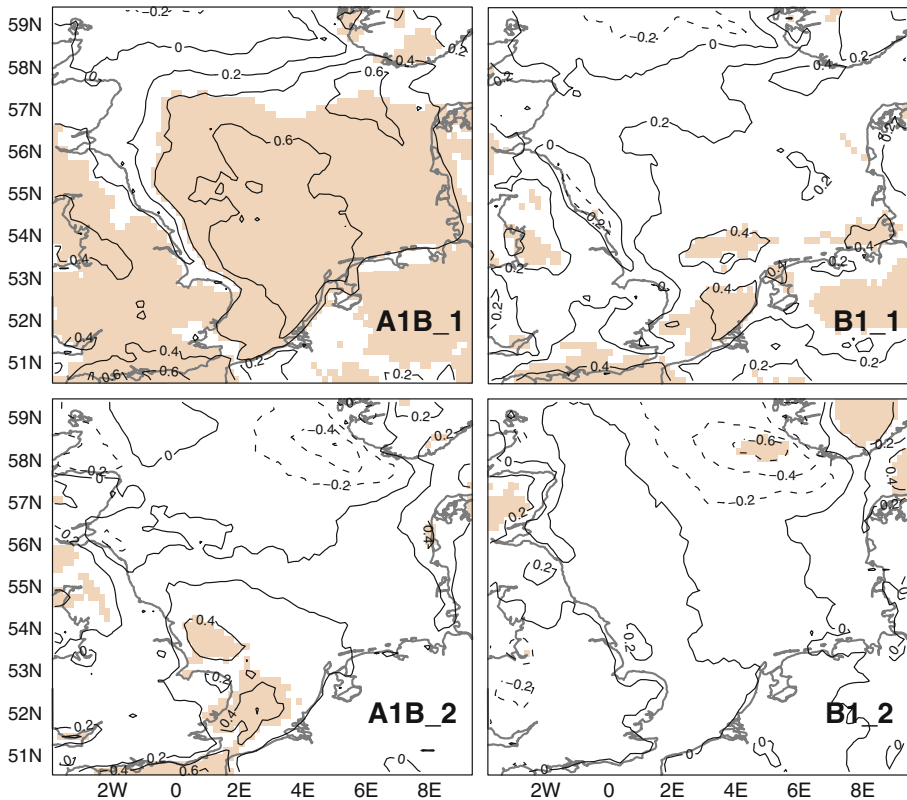


Fig. 4 Climate change signals Δ_{vi} for 30-year averages of annual 99 percentile wind speed in meters per second for A1B_1 (upper left), B1_1 (upper right), A1B_2 (lower left) and B1_2 (lower right). Shaded areas show significant differences on a 95% level based on a Student's *t* test

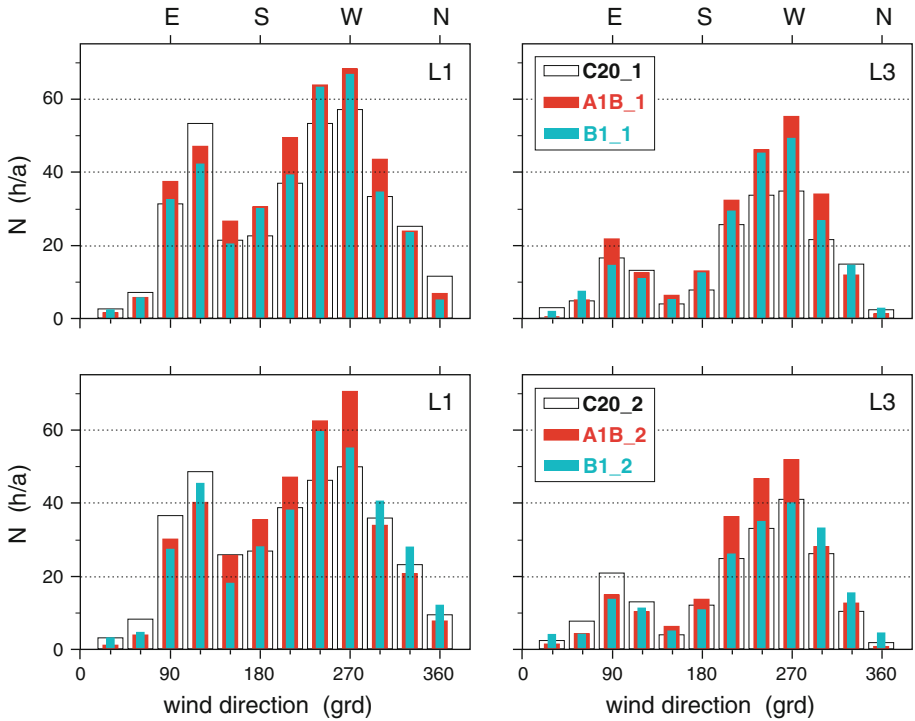


Fig. 5 Frequency distribution of wind directions for wind speeds greater than 17.2 m/s for 30-year slices of 6 realizations (C20: 1961–1990; A1B, B1: 2071–2100). 90°, 180°, 270° and 0°/360° correspond to E(ast), S(outh), W(est) and N(orth), respectively. For locations see Fig. 1

Skagerrak (+0.4 m/s) but for most parts of the North Sea changes in wind speed are between -0.1 and +0.1 m/s.

Generally, all four realizations show an increase in the mean annual 99 percentile of the wind speed for most parts of the North Sea. On a 95 %-level, these changes are only statistically significant (based on a Student’s *t* test) above roughly 0.4 m/s. Maximum changes can be found in almost all projections (except B1_2) in the southern North Sea including the German Bight. All projections show a decrease (not statistically significant) in the mean annual 99 percentile in the northern and northeastern North Sea.

To get a more general view of the four climate change realizations, Fig. 7 (left panel) shows the difference of the ensemble mean for the annual 99 percentile between the 30-year period 2071–2100 and the control period 1961–1990. These differences show an increase over sea of wind speeds of up to 0.3 m/s in the southern North Sea and the German Bight. Note that due to the larger sample size of the ensemble mean compared to the single realizations, already changes larger than 0.2 m/s are statistically significant on a 95 %-level.

For changes in surge levels in coastal areas, not only the wind speed itself is important, but also the frequency of strong winds and the wind direction. Generally, it has been found that the frequency of strong winds somewhat increases for the end of the twenty-first century (not directly shown here, but it can be derived from Fig. 8 which shows in the upper panels that the strong westerly winds increase more than the strong easterly winds

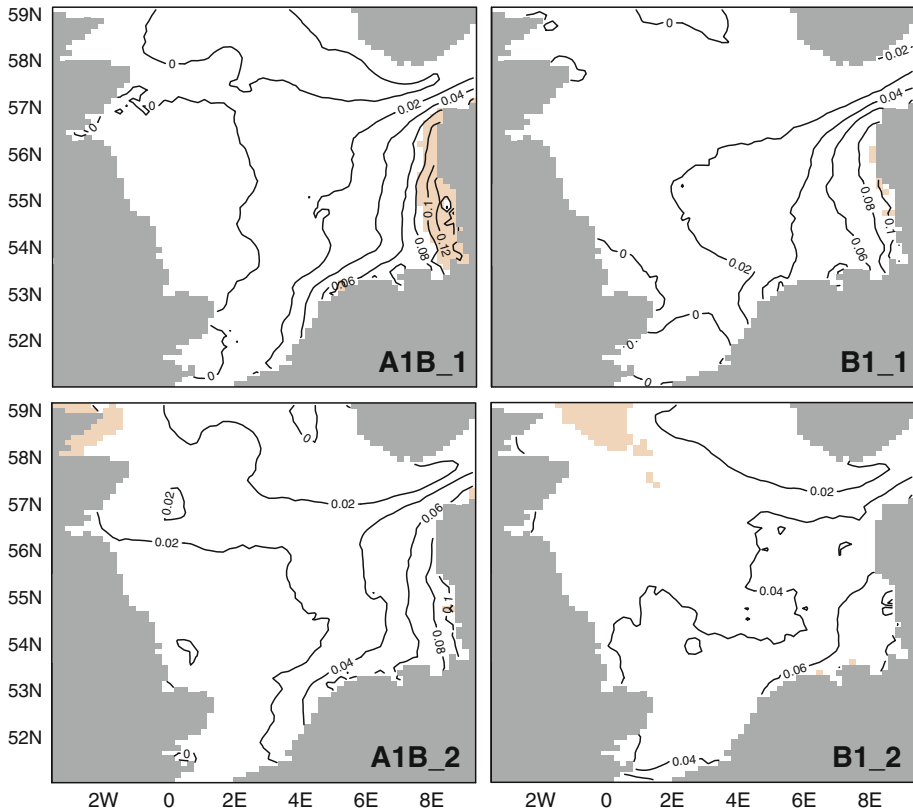


Fig. 6 Climate change signals Δ_{si} for 30-year averages of annual 99 percentile storm surge height in meters for A1B_1 (upper left), B1_1 (upper right), A1B_2 (lower left) and B1_2 (lower right). Shaded areas show significant differences on a 95% level based on a Student's t test

decrease). Changes in the wind direction for the end of the century are shown in Fig. 5. In particular, the frequency distributions for wind speeds stronger than 17.2 m/s are compared for the time slices 1961–1990 and 2071–2100. Both presented locations (L1 and L3) display a general increase in frequency of strong south-westerly to north-westerly winds and a small decrease of northerly and/or easterly winds. This tendency is evident for all four climate realizations with slight variations for the particular sectors.

3.2.2 Storm surge heights

The climate change signals for storm surge heights are presented in Fig. 6. The results for the four climate realizations are shown as differences between mean annual 99-percentiles for the future (2071–2100) and the reference (1961–1990) climate.

For all scenarios, the maximum increase in storm surge height occurs in the south-eastern North Sea. There is a gradual increase in the storm surge heights toward the Elbe estuary at the end of the twenty-first century. This corresponds to the general pattern of the storm surge height distribution for the North Sea, which has its maximum in the German Bight (not shown). The major and only statistically significant (95 %-level) differences (up

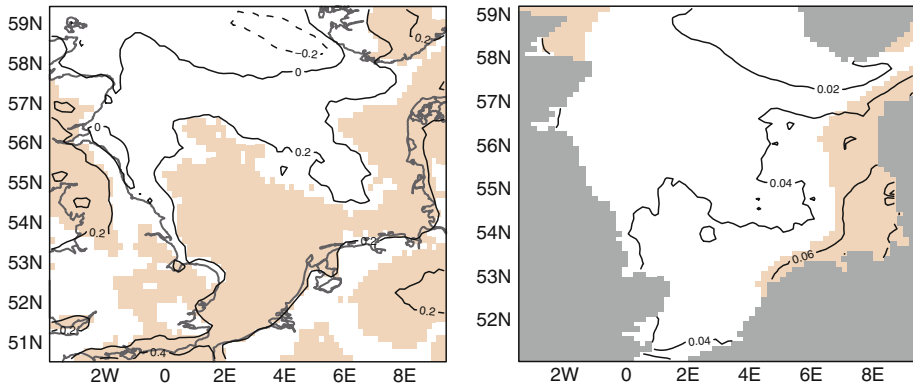


Fig. 7 Climate change signals for 30-year averages of annual 99 percentile wind speed (*left*) in meters per second and storm surge height (*right*) in meters for the ensemble mean. Shaded areas show significant differences on a 95% level based on a Student’s *t* test

to 13 cm) are found for the A1B_1 scenario, which is about 10 % increase compared to the control simulation values. For other scenarios, the changes reach up to 10 cm (approx. 8 % of the reference values). This is in agreement with the wind speed statistics (Fig. 4), which also show maximum changes for the A1B_1 scenario. Furthermore, it can be seen that the storm surge increase is more pronounced for the eastern German Bight (North Frisian Islands) and the Danish coasts than for the southern German Bight (East Frisian Islands) and the Netherlands coasts. This can be attributed to the prevailing westerly winds during storms and their increased frequency in the future climate realizations (Fig. 5), which cause increased wind set-up and thus more increased water levels in the east rather than in the south.

The patterns of the storm surge height deviations for the central and eastern North Sea vary between the four climate projections. In general, the changes are small, within +/-3 cm for the major parts of the North Sea, with the exception of the B1_2 scenario, where the changes are everywhere positive and reach 4–6 cm. Slightly negative changes are found in the northern part of the North Sea and along the southeastern British coast for the scenarios A1B_1 and B1_1. The differences of the ensemble mean are presented in Fig. 7 (right panel) and show a larger statistically significant area in the German Bight, but changes only range between 4 to 8 cm (approx. 5 % of the reference values).

3.3 Temporal variations of the climate change signals

The annual 99 percentiles of 140-year long time series (1961–2100) of wind speed and storm surge height at selected locations have been averaged for 111-year long series of 30-year time slices (running average from 1961–1990 to 2071–2100). Figure 8 displays climate change signals as deviations compared to 1961–1990 ensemble mean for each of the four realizations, as well as for the ensemble mean with the corresponding 95 % confidence interval defined with a bootstrapping method. These time series confirm the results based on the time slices for 2071–2100 to 1961–1990, shown before (see Figs. 4, 6, 7). These signals show a small increase toward 2071–2100, which vary spatially and among the four climate realizations. For the two locations in the German Bight (L2 and L3), the increase is strongest in the A1B_1 realization. Temporal variations of surge

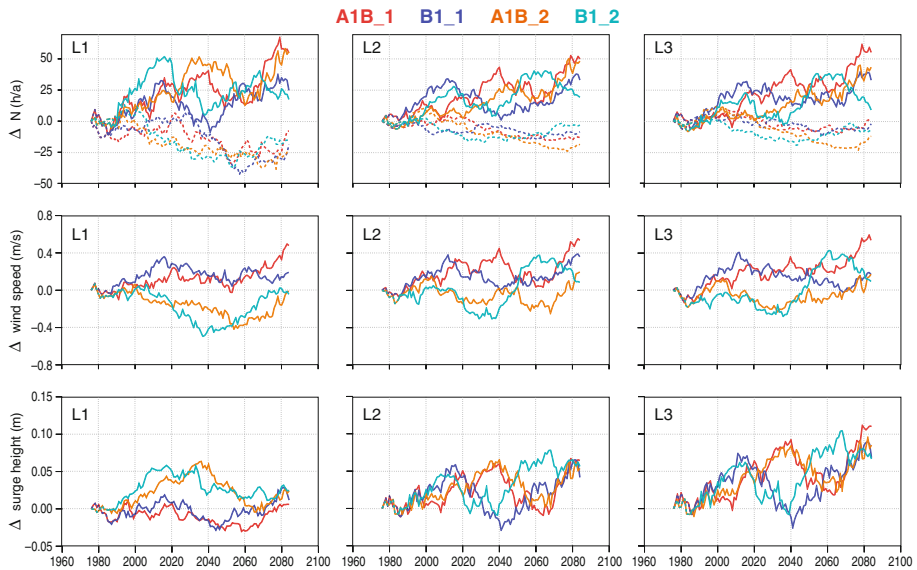


Fig. 8 Time series of climate change signals ΔN_{si}^{an} for 30-year running averages of annual frequencies of strong westerly ($165^\circ\text{--}345^\circ$, full lines) and easterly ($345^\circ\text{--}165^\circ$, dashed lines) winds (≥ 17.2 m/s) (top). Time series of climate change signals Δ_{si}^{an} for 30-year running averages of annual 99 percentile wind speed (middle) in meters per second and storm surge height (bottom) in meters for the four climate realizations at three selected areas. The respective ensemble mean time series are displayed by the thick black curve. Wind speed and surge height are plotted relative to the corresponding ensemble mean of the 30 year period 1961–1990. Shaded grey areas correspond to the 95 % confidence interval for the ensemble mean based on bootstrapping

heights cannot be directly related to the changes in local wind speed and/or direction (Fig. 8), as the combination of both is important. Furthermore, the history of the meteorological conditions has to be considered. However, there is a tendency that variations in the signals for the surge height are partly related to respective changes in the frequency of strong westerly winds.

Furthermore, the time series point out that there are fluctuations in between the time slices 1961–1990 and 2071–2100. They are in the same order of magnitude as or even stronger than the increase in 2071–2100 and represent the internal variability of the system. For example, the difference of the climate change signals between 2024–2054 and 2053–2083 periods at L3 is about 11 cm for the B1_2 realization, whereas the increase between 1961–1990 and 2071–2100 is only about 7 cm. Moreover, the time series show that the strongest increase of the signals must not necessarily occur toward the end of the twenty-first century: for location L3 and realization B1_2, the highest signal occurs, e.g., for the time slice 2053–2083. For location L1 in the central North Sea, changes are somewhat smaller, and the largest increases occur in the scenarios A1B_2 and B1_2 in the first half of this century.

The time series are given for the 99 percentiles, and it has to be mentioned that the patterns for other high percentiles (e.g., 99.5 or 99.9) look slightly different both in terms of internal variability as well as between the four climate realizations. For example, the 99 percentile for A1B_1 and A1B_2 show comparable inter-annual variations for L2 and L3, whereas the temporal variations for the 99.5 or 99.9 percentiles are different for these two

Table 1 Trends over the 140-year period 1961–2100 for the annual 99 percentile and the annual maximum surge height for the four climate projections and the ensemble mean for locations L2 (top) and L3 (bottom) together with the 95 % confidence interval (CI) and the significance (*) based on the *t* test

Climate projection	Annual 99 percentile surge height				Annual maximum surge height			
	Trend (cm/100a)	95 % CI (cm/100a)	Trend (%/100a)	TT	Trend (cm/100a)	95 % CI (cm/100a)	Trend (%/100a)	TT
L2								
A1B_1	5	±6	5.2		10	±15	5.5	
B1_1	3	±6	3.2		8	±15	4.4	
A1B_2	3	±6	2.6		0	±14	−0.1	
B1_2	5	±5	4.3		0	±16	0.06	
Mean	4	±4	3.8	*	2	±1	2.4	*
L3								
A1B_1	10	±6	8.2	*	14	±15	7.1	
B1_1	6	±6	4.6		10	±16	4.9	
A1B_2	5	±6	4.5		7	±15	3.3	
B1_2	6	±6	4.7		4	±16	1.8	
Mean	7	±3	5.5	*	9	±8	4.2	*

realizations (not shown here). The spatial distribution of the 99 percentile signals shown in Fig. 6 can also differ from those for the distributions of the, e.g., 99.5 or 99.9 percentile signals. It also has to be pointed out that the climate change signals of the storm surge height deviations can be different when compared with another control period (e.g. 1971–2000) or when other averaging intervals are used. However, the general pattern, i.e. smaller changes for the central North Sea and increased changes in the southeastern North Sea (German Bight) as well as decadal variations, persists.

In Table 1, linear trends in annual 99 percentile and maximum surge heights are listed for the four realizations as well as for the ensemble mean for the locations L2 and L3. The trends are small compared to the decadal variations and range between 3 to 10 cm/100a and between 0 and 14 cm/100a for the annual 99 percentile and the annual maximum surge heights, respectively. The largest trends with 10 and 14 cm/100a (8 and 7 %) are found for the A1B_1 scenario. These trends are statistically significant only for the ensemble mean and for the A1B_1 annual 99 percentile at L3.

The shown future increase in higher percentiles of the storm surge heights is more related to an increased frequency of high surge heights and less related to an increase in absolute water levels with respect to the present-day conditions (reference climate). Figure 9 shows exemplarily for the location L3 time series of the annual exceedance frequency over three threshold values: the 99.9, 99.99 percentiles and the maximum of the reference simulations for 1961–1990. Toward 2100, the future climate realizations, except B1_2, show a general increase in the exceedance frequency, but the maximum surge occurring in the respective reference simulation is only seldom surpassed: in three years in A1B_1 (in total 7 h out of 876576 h), in four years in B1_1 (16 h) and A1B_2 (20 h) and in eight years in B1_2 (42 h) within the time span 2001 to 2100. Scenario B1_2 shows a somewhat deviant behavior: the exceedances are highest in the 2010s to 2020s.

To describe severe changes between the future and the reference climates, 50-year return values for storm surge height have been estimated for the locations L2 and L3 (Fig. 10). Additionally, this figure displays respective return values for the absolute water

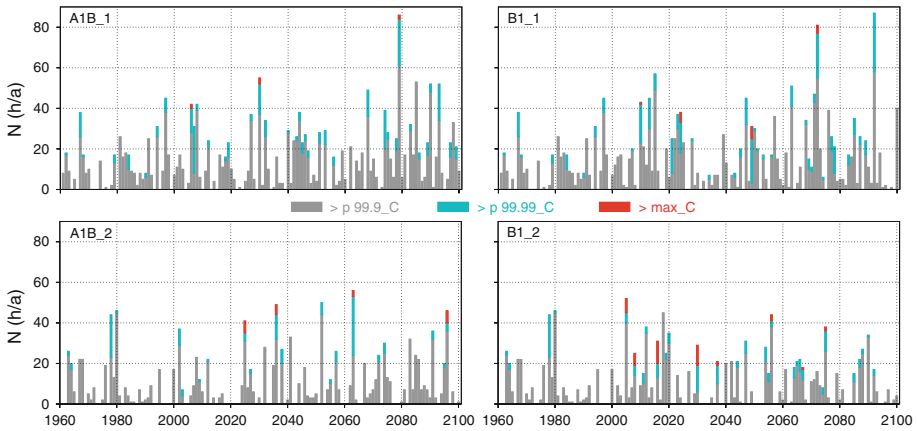


Fig. 9 Time series of the annual exceedance frequency of the storm surge height over 3 thresholds (99.9, 99.99 percentiles and maximum of the respective control period 1961–1990) for the four climate realizations exemplarily for L3

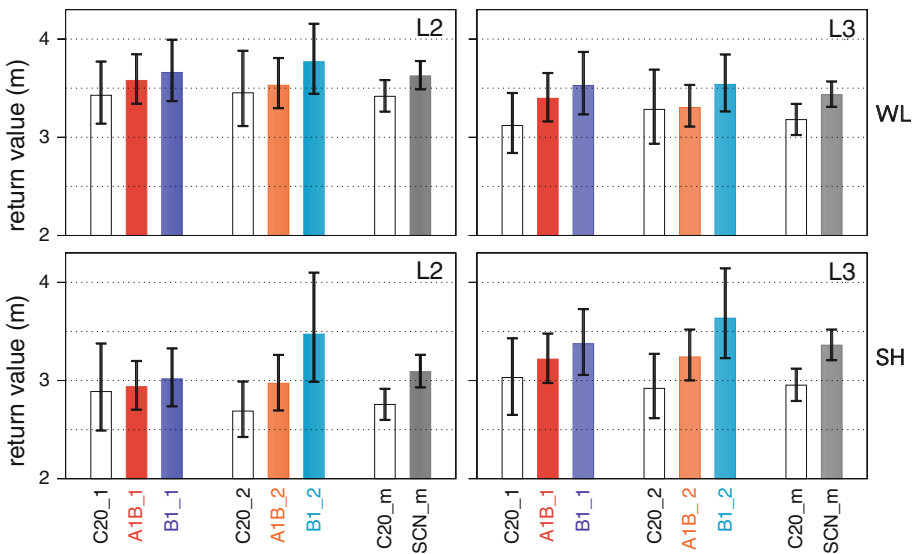


Fig. 10 50-year return values for water level (WL, upper panels) and surge height (SH, lower panels) for the control periods (C20_1 and C20_2) and the four future szenarios (A1B_1, B1_1, A1B_2, B1_2) as well as for the control mean (C20_m) and the scenario mean (SCN_m) for the locations L2 and L3. The 95 % confidence interval for each return value, based on a bootstrapping approach, is shown by the black bars

level which are more relevant with respect to e.g. coastal protection. The increase in the climate projections for both, water level and surge height, is in the order of 0.1 to 0.4 m except for B1_2. The increase of about 0.7 to 0.8 m for storm surge height in B1_2 is the only statistically significant increase within the four projections. In B1_2, the exceedance frequency for the threshold values based on the 99.9 and 99.99 percentiles is relatively small, but those for the maximum control surge is comparably high (see ig. 9). Also, the increase in the ensemble mean of 0.3 to 0.4 m for surge height is significant. Changes in

water level are somewhat smaller than those in surge height. This may be due to the fact that maximum surge is often not in coincidence with tidal high water. The locations L2 and L3 in the German Bight are about 20–50 km seawards of the coasts. Nearer to the coasts the described changes may be higher.

4 Discussion and Conclusion

The four climate realizations of future storm surge height show differences in both the amplitude and the spatial patterns for the climate change signals of the 30-year long time slices for 2071 to 2100. Nevertheless, all realizations show that larger and statistically significant changes are mainly limited to the southeastern part of the North Sea. There is an increase in storm surge height toward the coasts of the German Bight which is larger for the eastern coast (North Frisian Islands), where it reaches in one realization about 10 % of the reference climate storm surge heights, than for the southern coast (East Frisian Islands), where it is less than 8 %. The more reliable changes of the ensemble mean show an increase of about 5 % in the German Bight for the surge height. This is in coincidence with the increase in frequency of stronger southwesterly and westerly winds (≥ 17.2 m/s) which enhance the wind-setup toward the east. This shift to more westerly winds is consistent with results from Pinto et al. (2007), who found in the underlying future global climate simulations, an increase of the North Atlantic storm track activity and a shift to a more zonal mean flow.

In general, these climate change signals toward the end of the twenty-first century (2071–2100) are comparable to those from four realizations with wind and pressure fields based on model/scenario combinations with the two IPCC scenarios A2 and B2 and two different global models (Woth 2005; Woth et al. 2006; Weisse et al. 2009). The magnitude of the signals are not directly comparable to those presented for the A1B and B1 realizations in the present study. Nevertheless, the A2 and B2 realizations show also an increase in the southeastern North Sea and some decrease at some parts off the British coast and in the northern North Sea. Whereas the signals vary between the eight future climate realizations in their magnitude and spatial distribution, there is agreement among the realizations about the sign of the signal for the German Bight: all of them show an increase in storm surge height toward the coasts for 2071–2100 compared to 1961–1990.

The availability of the transient simulations enables the analysis of time series. This analysis for chosen areas within the North Sea displays that the climate change signals for the four climate realizations for A1B and B1 vary not only spatially and between the realizations but also in time. Whereas the time series for the areas in the southeastern North Sea show a general increase in storm surge height toward 2100 in all four projections, they also reveal that the largest signals (strongest increase) must not necessarily occur at the end of the century, but can locally occur in between the time period 2001–2100 in some of the climate projections. Also, local negative changes have been detected throughout the twenty-first century (e.g., for L2, the differences vary between -3 and $+8$ % of the reference storm surge magnitudes; for L3, they vary between -2 and $+10$ %). Thus, there is no continuous increase or decrease in the storm surge heights toward the year 2100. The decadal variations within a single realization as well as between the four realizations are in the same order of magnitude as the climate change signals for the end of the century (2071–2100). Temporal variations of the 99 percentile surge height are comparable to those of the NAO index derived by Pinto et al. (2007) with the same global simulation. Hence, the changes in the surge climate are partly related to the large atmospheric conditions.

The changes in storm surge height are mainly due to respective changes in the frequency of higher surge heights (e.g. ≥ 99 and 99.9 percentiles). In the four future projections, exceedances of surge heights over the maximum surge height of the respective control period (1961–1990) are rare. The 50-year return values for the annual maximum ensemble mean surge heights show that changes could be in the order of +0.4 m during single events. In the scenario B1_2 in which the maximum surge heights of the reference period are more often exceeded, the 50-year return values range up to about 0.7 m for L2 and up to about 0.8 m for L3. The return values are generally in the same order of magnitude as given in Lowe and Gregory (2005). The selected locations (L2, L3) are more than 20 km off the coasts; thus, near or at the coasts of the southeastern North Sea, changes in storm surge height are likely to be higher.

The analysis of the 140-year long climate realizations has displayed that not only uncertainties due to models and emission scenarios have to be taken into account in climate impact research but also uncertainties due to initial conditions presenting the natural internal variability. This is also described in Weidemann (2009) and summarized in Weisse et al. (2011). The study by Weidemann (2009) is based on statistical downscaling of 17 realizations for the scenario A1B only differing by varying initial conditions displays a wide range of trends (from -0.08 to 0.18 m for the German Bight) over the years 1958–2100. The trends shown in this study for the A1B and B1 projections are well within the range given by Weidemann (2009).

Summarizing, the uncertainties in climate change impact estimations due to models and scenarios are enhanced by uncertainties due to initial conditions and to the respective time spans under consideration. In the scenario/ initial condition combinations investigated in this study, the scenario-induced differences between the climate change signals are in the same order of magnitude as those based on different initial conditions. Note that this study is only based on four realizations, and for a more general statement on possible changes of the surge climate in the twenty-first century, a larger ensemble (more initial conditions, different GCMs and RCMs) is needed. Based on this study together with previous studies, it can be expected that despite the remaining uncertainties toward the end of this century extreme surge heights are likely to show a small increase toward the coasts of the German Bight with stronger changes along the North Frisian Islands in case of anthropogenic climate change. This increase is superimposed by strong decadal variability; and thus, the largest increase must not necessarily occur at the end of the century. A rise in mean sea level, not included in the present study, is expected to take place more steadily and may reach its local maximum at the end of the considered time period. Thus, especially at the end of the century, it can become at least as important as the meteorologically induced water-level changes. Human activities in the German Bight and along its coasts may be confronted with more frequent surge-induced impacts throughout the twenty-first century.

Acknowledgments The authors are thankful to H. Kapitza and E.M.I. Meyer for assistance with the TRIM-NP model and to Ms. Gardeike for assistance with the graphics. The investigation was partly supported in the context of the joint projects A-KÜST in KLIFF (Förderkennzeichen VWZN2455, Az. 99-22/07) and KLIMZUG-NORD (Förderkennzeichen 01LR08051).

References

- Beniston M, Stephenson DB, Christensen OB, Ferro CAT, Frei C, et al (2007) Future extreme events in European climate: an exploration of regional climate model projections. *Clim Change* 81:71–95 doi: [10.1007/s10,584-006-9226-z](https://doi.org/10.1007/s10,584-006-9226-z)

- Brown JM, Wolf J, Souza AJ (2010) Surge modelling in the eastern Irish sea: present and future storm impact. *Ocean Dyn* 60:227–236. doi:[10.1007/s10236-009-0248-8](https://doi.org/10.1007/s10236-009-0248-8)
- Brown JM, Souza AJ, Wolf J (2011) Past to future extreme events in Liverpool Bay: model projections from 1960–2100. *Clim Change*. doi:[10.1007/s10584-011-0145-2](https://doi.org/10.1007/s10584-011-0145-2)
- Casulli V, Cattani E (1994) Stability, accuracy and efficiency of a semi-implicit method for three-dimensional shallow water flow. *Comput Math Appl* 27(4):99–112
- Debernard JB, Røed LP (2008) Future wind, wave and storm surge climate in the Northern Seas: a revisit. *Tellus* 60:427–438. doi:[10.1111/j.1600-0870.2008.00312.x](https://doi.org/10.1111/j.1600-0870.2008.00312.x)
- Debernard JB, Sætra Ø, Røed LP (2002) Future wind, wave and storm surge climate in the Northern Seas. *Climate Res* 23:39–49
- Hollweg H, Böhm U, Fast I, Hennemuth B, Keuler K, Keup-Thiel E, Lautenschlager M, Legutke S, Radtke K, Rockel B, Schubert M, Will A, Woldt M, Wunram C (2008) Ensemble simulations over Europe with the regional climate model CLM forced with IPCC AR4 global scenarios. Technical report 3, Support for Climate- and Earth System Research at the Max Planck Institute for Meteorology, ISSN 1619–2257
- Houghton JT, Ding Y, Griggs DJ, Noguer M, van der Linden PJ, Dai X, Maskell K, Johnson CA (eds) (2001) *Climate Change 2001: The Scientific Basis. Contribution of Working Group I to the Third Assessment Report of the Intergovernmental Panel on Climate Change*. Cambridge University Press, Cambridge, UK, 881 pp
- Howard T, Lowe J, Horsburgh K (2010) Interpreting century-scale changes in southern North Sea storm surge climate derived from coupled model simulations. *J Climate* 23:6234–6247. doi:[10.1175/2010JCLI3520.1](https://doi.org/10.1175/2010JCLI3520.1)
- Kapitza H (2008) Mops: a morphodynamical prediction system on cluster computers. In: Laginha JM, Palma M, Amestoy PR, Dayde M, Mattoso M, Lopez J (eds) *High performance computing for computational science-VECPAR 2008, Lecture Notes in Computer Science*, Springer, pp 63–68
- Kapitza H, Eppel DP (2000) Simulating morphodynamical processes on a parallel system. In: Spaulding ML, Butler HL (eds) *Estuarine and coastal modeling*. American Society of Civil Engineers, New York, pp 1182–1191
- Lionello P, Nizzero A, Elvini E (2003) A procedure for estimating wind waves and storm-surge climate scenarios in a regional basin: the Adriatic Sea case. *Climate Res* 23:217–231
- Lowe JA, Gregory JM (2005) The effects of climate change on storm surges around the United Kingdom. *Phil Trans Roy Soc A* 363:1313–1328
- Lyard F, Lefevre F, Letellier T, Francis O (2006) Modelling the global ocean tides: modern insights from FES2004. *Ocean Dyn* 56:394–415
- Marsland SJ, Haak H, JungCLAUS JH, Latif M, Röske F (2003) The Max-Planck-Institute global ocean/sea ice model with orthogonal curvilinear coordinates. *Ocean Model* 5:91–127
- Nakicenovic N, Swart R (eds) (2000) *Special Report on Emissions Scenarios. A Special Report of Working Group 3 of the Intergovernmental Panel on Climate Change*. Cambridge University Press, Cambridge, UK, 599 pp
- Pinto JG, Ulbrich U, Leckebusch GC, Spanghel T, Reyers M, Zacharis S (2007) Changes in the storm track and cyclone activity in the three SRES ensemble experiments with the ECHAM5/MPI-OM1 GCM. *Clim Dyn* 29:195–210. doi:[10.1007/s00382-007-0230-4](https://doi.org/10.1007/s00382-007-0230-4)
- Rockel B, Will A, Hense A (eds) (2008) *Special issue regional climate modeling with COSMO-CLM (CCLM)*, vol 17. *Met. Zeitschrift*
- Röckner E, Bäuml G, Bonaventura L, Brokopf R, Esch M, Giorgetta M, Hagemann, Kirchner I, Kornblüeh L, Manzini E, Rhodin A, Schlese U, Schulzweida U, Tompkins A (2003) The atmospheric general circulation model echam5. Part i: model description. *Mpi-rep* 349, Max Planck Institute for Meteorology
- Sterl A, van den Brink H, de Vries H, Haarsma R, van Meijgaard E (2009) An ensemble study of extreme storm surge related water levels in the North Sea in a changing climate. *Ocean Sci* 5:369–378
- Weidemann H (2009) *Statistisch regionalisierte Sturmflutszenarien für Cuxhaven*. Diploma Thesis, Christian-Albrechts-Universität zu Kiel, 99 pages
- Weisse R, Pluess A (2006) Storm-related sea level variations along the north sea coast as simulated by a high-resolution model 1958–2002. *Ocean Dyn* 26:16–25
- Weisse R, von Storch H, Callies U, Chrastansky A, Feser F, Grabemann I, Günther H, Plüss A, Stoye T, Tellkamp J, Winterfeldt J, Woth K (2009) Regional meteorological-marine reanalysis and climate change projections. Results for northern Europe and potential for coastal and offshore applications. *Bull Am Met Soc* 90(6):849–860. doi:[10.1175/2008BAMS2713.1](https://doi.org/10.1175/2008BAMS2713.1)
- Weisse R, von Storch H, Niemeier HD, Knaack H (2011) Changing north sea storm surge climate: an increasing hazard? *Ocean Coast Manage*. doi:[10.1016/j.ocecoaman.2011.09.005](https://doi.org/10.1016/j.ocecoaman.2011.09.005)

- Woth K (2005) North Sea storm surge statistics based on projections in a warmer climate: How important are the driving GCM and the chosen emission scenario? *Geophys Res Lett* 32: L22,708 doi: [10.1029/2005GL023762](https://doi.org/10.1029/2005GL023762)
- Woth K, Weisse R, von Storch H (2006) Climate change and North Sea storm surge extremes: an ensemble study of storm surge extremes expected in a changed climate projected by four different regional climate models. *Ocean Dyn* 56(1):3–15. doi: [10.1007/s10236-005-0024-3](https://doi.org/10.1007/s10236-005-0024-3)